

Measuring the Complexity of Ultra-Large-Scale Adaptive Systems

Michele Amoretti¹, Carlos Gershenson²

¹ Centro Interdipartimentale SITEIA.PARMA,
Università degli Studi di Parma, Italy
Parco Area delle Scienze 181a, 43124 Parma, Italy
email: michele.amoretti@unipr.it

phone: +39 0521 906147

fax: +39 0521 905723

² Computer Science Department, IIMAS,
Universidad Nacional Autónoma de México

November 19, 2021

Abstract

Ultra-large scale (ULS) systems are becoming pervasive. They are inherently complex, which makes their design and control a challenge for traditional methods. Here we propose the design and analysis of ULS systems using measures of complexity, emergence, self-organization, and homeostasis based on information theory. These measures allow the evaluation of ULS systems and thus can be used to guide their design. We evaluate the proposal with a ULS computing system provided with adaptation mechanisms. We show the evolution of the system with stable and also changing workload, using different fitness functions. When the adaptive plan forces the system to converge to a predefined performance level, the nodes may result in highly unstable configurations, that correspond to a high variance in time of the measured complexity. Conversely, if the adaptive plan is less "aggressive", the system may be more stable, but the optimal performance may not be achieved.

1 Introduction

Ultra-large-scale (ULS) systems [1] are the result of the interconnection of heterogeneous IT systems — characterized by decentralized goals and control — that as a whole exhibit one or more properties (*i.e.* behavior) which are not easily inferred from the properties of the individual parts. ULS are complex systems, since the interactions of their components determine their future state and that of the system [2]. This interconnectedness limits the predictability of ULS, since interactions generate novel information, thus making traditional methods that rely on prediction inadequate [3].

Examples of ULS systems are the Internet, healthcare infrastructures, e-markets, global ambient intelligence systems, and distributed high-performance computing facilities. To overcome the rapidly growing complexity of their management, and to reduce the barrier that complexity poses to further growth, a variety of architectural frameworks based on “self-regulating” components has been proposed [4, 5]. Adaptive plans may turn ULS systems into a more efficient, environment-driven systems, provided that the adaptive plan itself does not introduce further complexity and instabilities [6].

Even when there are several examples of ULS and the importance of their adaptivity is well accepted, there is no standard method for developing adaptive ULS. Even more, there is no framework to measure how adaptive different ULSs are. In this paper, we propose the evaluation of adaptive ULS using complexity measurement principles introduced by Gershenson and Fernandez in [7]. We apply these to a peer-to-peer system designed with the Distributed Remodeling Framework (DRF) defined by Amoretti in [8]. Our contribution lies in the proposal of a methodology to measure the adaptivity of any ULS, facilitating their comparison.

To the best of our knowledge, this is the first proposal of a general methodology for measuring the complexity of ULS systems, independent of the particular implementation. Usually, benchmarks are adopted to test the characterize single parts of ULS systems (which are always built with a bottom-up approach), and partial indicators are used to analyze the whole system in simulation *et al.* [9].

The paper is organized as follows: In the following section, related work concerning ULS evolutionary systems is mentioned. In section 3, the proposed methodology is presented. In section 4, the case study of an ULS peer-to-peer computing system with distributed genetic adaptation is used as an illustration. In section 5, results of the case study evaluation carried

out by means of discrete event simulation are shown. Section 6 concludes the paper with a summary of achieved results and an outline of future work.

2 Related Work

2.1 ULS Systems

The SEI study [1] on ULS systems brings together experts in software and other fields to examine the consequences of rapidly increasing scale in software-reliant systems. The report details a broad, multi-disciplinary research agenda for developing the ultra-large-scale systems of the future, that also include computer-supported evolution, adaptable structure and emergent qualities.

All these aspects can be placed under the umbrella of autonomic computing, that proposes to provide distributed systems with four key properties: self-configuration, self-healing, self-optimization, and self-protection [10]. IBM has suggested a reference model for autonomic control loops, which is sometimes called the MAPE-K (Monitor, Analyze, Plan, Execute, Knowledge) loop [11]. This model is being widely used to communicate the architectural aspects of autonomic systems. The MAPE-K construction can be iterated, as the control loop itself could be adaptive (see for example [12] and [13]).

Nakano and Suda have proposed a distributed approach for evolutionary adaptation of network services [14], based on agents that migrate, replicate, reproduce and die. An agent invokes its behavior based on its internal state and environmental conditions, using a weighted sum aggregation method. For example, when the weighted sum for reproduction exceeds its reproduction threshold, the agent selects a reproduction partner from agents that are within n hops.

Hales introduced an algorithm called SLAC, which means selfish link and behavior adaptation to produce cooperation [15]. SLAC is based on the copy and rewire approach, whose basic algorithm assumes that peer nodes have the freedom to change the way they handle and dispatch requests to and from other nodes, and drop and make links to nodes they know about. Another interesting approach for node restructuring has been proposed by Tyson *et al.* [16], that show how survival of the fittest has been implemented into the Juno middleware. On receipt of a superior component, Juno dynamically reconfigures the internal architecture of the node, by replacing the existing

component with the new one.

2.2 Peer-to-Peer Networks

Distributed control is the main reason for the intrinsic *robustness* and *resiliency* of complex adaptive systems. Actually, they are relatively insensitive to perturbations or errors, and have a strong capacity to restore themselves. Due to their distributed organization, the non-damaged regions can usually make up for the damaged ones.

Distributed control is also a characterizing aspect of peer-to-peer (P2P) networks [17, 18, 19, 20, 21], where every node (the peer) acts as server and client, by collecting, providing and consuming resources (such as CPU cycles, storage, and bandwidth). A P2P network is usually an overlay network which builds over existing physical infrastructures. Some overlay schemes (such as those of the DKS family [22]) lead to high scalability, efficient resource sharing mechanisms and robustness to node failure. The drawbacks are that administration may be difficult (one person cannot determine the whole accessibility setting of the whole network), malicious software can be easily transmitted, and in general both normal functioning and recovery protocols must be based on distributed algorithms, by taking into account that emergent behaviors are difficult to predict.

P2P networks are complex, but distributed control is not sufficient for considering them adaptive. Usually, the peers have a static structure and execute prefixed protocols. To improve the efficiency of peer-to-peer systems while adapting to changing environmental conditions, static peer-to-peer protocols can be replaced by *adaptive plans*. Indeed, the introduction of artificial evolution in peer-to-peer networks allows to face environmental needs preserving high performance, while saving resources in a totally unsupervised manner. In a seminal paper on this topic, Paechter *et al.* call this concept *infoworld evolution* [23].

Evaluating the complexity of distributed adaptive systems, such as P2P networks, is a challenging task. Even more challenging is to exploit complexity measurements for improving the design of such systems.

2.3 Complexity Measurement

There are dozens of measures of complexity. Several of them are based on information theory [24]. This is convenient because anything can be measured

in terms of information, thus these measures can be applied to any studied phenomenon. Some measures of complexity correlate with “disorder” or “chaos”, making random phenomena to have the highest complexity. However, other approaches consider complexity as a balance between chaos and order. This balance is desirable for computing and living systems, since they require certain stability but also certain variability. The ordered extreme is robust, but does not enable adaptation. The chaotic extreme allows for adaptation and exploration, but information cannot be lost. The best possible adaptation can only occur in the critical regime between ordered and chaotic dynamics [25, 26]. In this approach, complexity is seen as a balance between propagating and transforming information [27]. Thus, systems with a higher complexity will be more adaptable than those which are not.

3 Methodology

The ULS systems we want to characterize are made of several thousands nodes that interact in a peer-to-peer fashion, *i.e.* without a centralized control. To describe the functional architecture and behavior of such nodes, we use the Distributed Remodeling Framework (DRF) [8]. Each peer has a modular structure that can dynamically change, by adding or removing components. Being p the total number of component types for the system, we define a vector \mathbf{M} of $q \leq p$ components, called the *model* of the peer. An adaptive plan τ produces a sequence of configurations, *i.e.* a trajectory through the *search space* \mathcal{M} of models, following an evolutionary process.

By means of the framework introduced by Gershenson and Fernandez in [7], we measure the evolution over time of the information I associated to \mathbf{M} , when the components of the latter are integer values $x \in [1..n]$ used as parameters for the node’s functional processes. Taking into account the latest W configurations of \mathbf{M} , we measure the frequency of each value for $x \in [1..n]$. Then we use the frequency as $P(x)$ and compute the normalized information as

$$I = \frac{-\sum P(x) \log_2 P(x)}{I_{max}} \quad (1)$$

where $I \in [0, 1]$ and $I_{max} = -\log_2 1/n$, since the maximum information value is achieved when all values $1, \dots, n$ have the same probability [7]. Minimum information ($I = 0$) occurs when only one value is repeated in time.

This implies that the node is static, i.e. there is no change.

For example, if the latest $W = 3$ configurations of \mathbf{M} have been $(1, 3, 5)$, $(1, 3, 6)$, $(1, 4, 6)$, then the frequencies are $P(1) = 1/3$, $P(2) = 0$, $P(3) = P(6) = 2/9$, $P(4) = P(5) = 1/9$. The associated information is

$$I = \frac{-1/3 \log_2 1/3 - 4/9 \log_2 2/9 - 2/9 \log_2 1/9}{-\log_2 1/6} = 0.85$$

Since peers are randomly initialized, we assume a random “input” and use the following simplified formulas [7]:

$$\text{emergence } E = I \tag{2}$$

Higher emergence implies that the process *produces* more information. Low emergence implies that the process does not produce information, i.e. $I = 0$.

$$\text{self-organization } S = 1 - I \tag{3}$$

In this simplified equation, self-organization can be seen as the opposite of emergence, as organization can be seen as a reduction of entropy [28], which is equivalent to I . Low emergence implies high self-organization and vice versa. The most self-organized process is that which is static, while the least self-organized process is that which changes the most, i.e. it is the most emergent ($I = 1$).

$$\text{complexity } C = 4 \cdot E \cdot S \tag{4}$$

where the 4 factor is for normalization reasons, since $I \in [0, 1]$ and C is maximized when $I = E = S = 0.5$. Complexity here is seen as a balance between emergence (change) and self-organization (order). Complexity is low when E or S are high, while it is maximal when they are equal.

$$\text{homeostasis } H = 1 - d(I, I_{init}) \tag{5}$$

where d is the normalized Hamming distance between the \mathbf{M} associated to I and I_{init} , which is the information associated to the initial configuration of the peer. H is a complementary measure of change in the system. The highest $H = 1$ is given when there is no change, $H \approx 1/n$ indicates lack of correlation between compared states.

A high E , S or H implies low adaptivity, since a system with high E implies constant change (close to noise), while high S and H imply a static system, which cannot adapt to changes in its demand. A high C implies adaptivity of the system.

4 Case study

We use the example of an ultra-large-scale computing system where nodes form a peer-to-peer overlay network, whose global functioning is the result of the interactions among nodes, and depends on their local evolution based on an adaptive plan implemented as a genetic algorithm (GA). Such a case study is particularly interesting because of the self-adaptation properties of the considered system. Our analysis shows that adaptive plans, being more or less "aggressive", can lead to very different results. The design of such systems requires to find a good tradeoff between stability and optimality of performance. Such a challenging task can be effectively supported by the complexity measurement methodology defined above.

In the considered system, shared resources cannot be acquired by replication once discovered, but may only be directly used upon contracting with their hosts. An example of such resources is disk space, which can be partitioned and allocated to requestors for the duration of a task, or in general for an arranged time.

The topology of the envisioned ultra-large-scale system can be represented as an undirected graph whose arcs stand for mutual knowledge among peers. The node degree k is the number of neighbors of each node. Its statistical distribution depends on the history and on the dynamics of the network, and may affect the performance of the distributed algorithms which are executed.

Every peer executes Algorithm 1, which is based on *epidemic* query propagation [29], to search for resources. Lookup messages are matched with local resources and, if necessary, propagated to neighbor peers. Every peer is provided with a cache that contains the descriptors of the remote resources that have been previously discovered. Such a cache is inspected before sending random (*i.e.* blind) queries. Lookup messages have a time-to-live (T), which represents the remaining number of hops before expiration. Every peer caches received queries, in order to drop subsequent duplicates. The reason of such an approach for resource lookup is that bio-inspired epidemic protocols are scalable and robust against network failures, while providing probabilistic

reliability guarantees [30].

Algorithm 1 Resource lookup

```

1: if resource is locally available then
2:   notify interested peer
3:   if interested peer still interested then
4:     provide resource instance to interested peer
5:   end if
6: else
7:    $T \leftarrow T - 1$ 
8:   if resource descriptor is in cache then
9:     propagate query to cached peer
10:  else
11:    if  $T > 0$  then
12:      propagate query to (all or some) neighbors
13:    end if
14:  end if
15: end if

```

Resource lookup is affected by the following parameters:

- f_k = fraction of neighbors targeted for query propagation
- T_{max} = propagations depth, *i.e.* the maximum number of times a query is forwarded by the peers before being removed from the network
- D_{max} = maximum size of the cache

that contribute to the definition of the peer’s phenotype:

$$\Phi \doteq \phi_0 f_k + \phi_1 T_{max} + \phi_2 D_{max} \tag{6}$$

In the previous formula, the constant weights $\phi_0, \phi_1, \phi_2 \in \mathbb{R}$ control the influence of each parameter. Such weights are set in advance to define the priorities of the three components of Φ . Of course one could set them to 1 and let such priorities emerge from the evolution of the genotype (defined below).

In traditional epidemic algorithms, the parameters have fixed values, and are set in advance according to the results of some tuning process, which should guarantee good performance with high probability. Actually, if all peers were configured with $f_k = 1$ and the same T value, the resulting scheme

would match the Gnutella protocol [31]. The purpose of introducing artificial evolution of these peers is to guarantee high system performance, while avoiding overabundant resource lookup messaging within the network. In the adaptive approach, the three parameters listed above are made functions of the chromosome, and are randomly initialized when a peer is created and joins the network. Moreover, such parameters are adaptively tuned, according to a fitness function F that is to be minimized, taking into account the average *query hit ratio*:

$$\langle QHR \rangle = AQ(QHR_0, \dots, QHR_k) = \frac{1}{k+1} \sum_{j=0}^k QHR_j \quad (7)$$

The query hit ratio is defined as the number of query hits QH , *i.e.* successful lookups, versus the number of submitted queries Q . In the previous equation, it is assumed that $j = 0$ for the considered peer, and $j = 1, \dots, k$ for its neighbors.

An increasing request rate penalizes the lookup performance, because the shared resources (*e.g.* CPU, RAM, disk space) are consumable. Thus, the fitness function must drive the peer in adapting its lookup parameters to the rate of direct or indirect user requests. Each peer applies the adaptive plan to its current model, and evolution can be either autonomous or based on the interaction with the peers' neighbors. In this case study, the second approach was adopted: each peer evolves its model by taking into account its neighbors' models (see below Algorithm 2).

Every peer is characterized by a model \mathbf{M} (genotype), defined by three genes $\{M_0, M_1, M_2\}$ with values in a limited subset of \mathbb{N} . The following equations define the mapping between the phenotype and genotype:

- $f_k = c_0 M_0$
- $T_{max} = c_1 M_1$
- $D_{max} = c_2 M_2$

where $c_i \in \mathbb{R}$, (with $i = 0, 1, 2$) are constants.

4.1 Fitness functions

Examples of suitable fitness functions are:

$$\begin{aligned}
 F_1(\Phi, \langle QHR \rangle) &= \begin{cases} 1/\Phi & \text{if } \langle QHR \rangle < \beta \\ \Phi & \text{if } \langle QHR \rangle > \beta \end{cases} \\
 F_2(\Phi, \langle QHR \rangle) &= (1 - \langle QHR \rangle) \frac{1}{\Phi} + \langle QHR \rangle \Phi \\
 F_3(\Phi, \langle QHR \rangle) &= \left(\frac{1}{\langle QHR \rangle + \delta} - 1 \right) \frac{1}{\Phi} + \langle QHR \rangle \Phi \\
 F_4(\Phi, \langle QHR \rangle) &= \left(\frac{\langle QHR \rangle}{\beta} - 1 \right) \left(\frac{\Phi}{\Phi_M} \right) + (1 - \langle QHR \rangle)
 \end{aligned}$$

where β is a threshold value, δ is a small parameter for avoiding division by zero when $\langle QHR \rangle = 0$, and $\Phi_M = \max\{\Phi\}$.

These fitness functions favor lower phenotypes when the average query hit ratio $\langle QHR \rangle$ is high, and higher ones when the $\langle QHR \rangle$ is low. If the values of the parameters which define the phenotype increase, the search process becomes more expensive in terms of time/space, but at the same time the probability of successful lookup (approximated by QHR) should be improved.

F_1 and F_4 allows to set a threshold β for $\langle QHR \rangle$, under which the M_i are forced to grow. Conversely, when $\langle QHR \rangle > \beta$ the M_i are forced to decrease. Conversely, F_2 and F_3 does not allow to set a threshold for $\langle QHR \rangle$. In the following of the article, we focus on F_2 and F_4 (illustrated in Figure 1), which are representative of the two approaches.

4.2 Adaptive plan

The logical operation of the peer is illustrated by the block diagram in Fig. 2. The resource lookup process is executed in a separate thread with respect to the adaptation process. However, they influence each other.

Algorithm 2 describes the adaptation process which is executed by each peer, with period T_a . The "best" neighbor is chosen according to a *fitness-proportionate selection* scheme, where the chance of a neighbor's model to be selected is inversely proportional to its fitness value. Cross-over is always performed, with a randomly-generated crosspoint. Mutation depends on $\langle QHR \rangle$, being highly improbable when the $\langle QHR \rangle$ of the peer and its

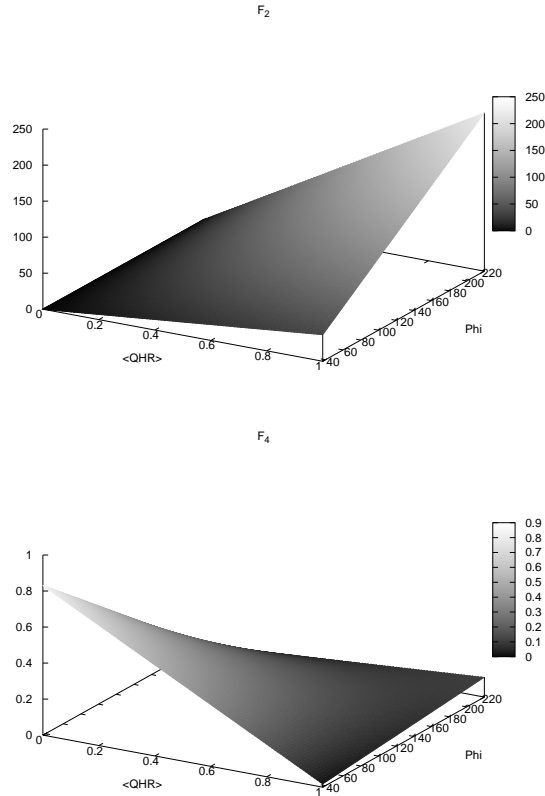


Figure 1: Plot of F_2 and F_4 with the parameters' values of the simulation experiments.

neighbors tends to 1. In general, the QHR may be less than 1 for different reasons. In particular circumstances, no resource may be available even if search messages are deeply and widely propagated. Also the chromosome of the current peer or the mutated offspring is then chosen using fitness-proportionate selection. Its consequence is that there is a chance some weaker solutions may survive the selection process.

This approach recalls Evolvable Agent (EvAg) [32], which is an evolutionary algorithm that structures its population by means of a gossiping protocol. Like in Algorithm 2, each peer is responsible for one solution, which is obtained by combining those of the first neighbors. For the sake of precision, in Algorithm 2, the peer's actual solution is also recombined with those of

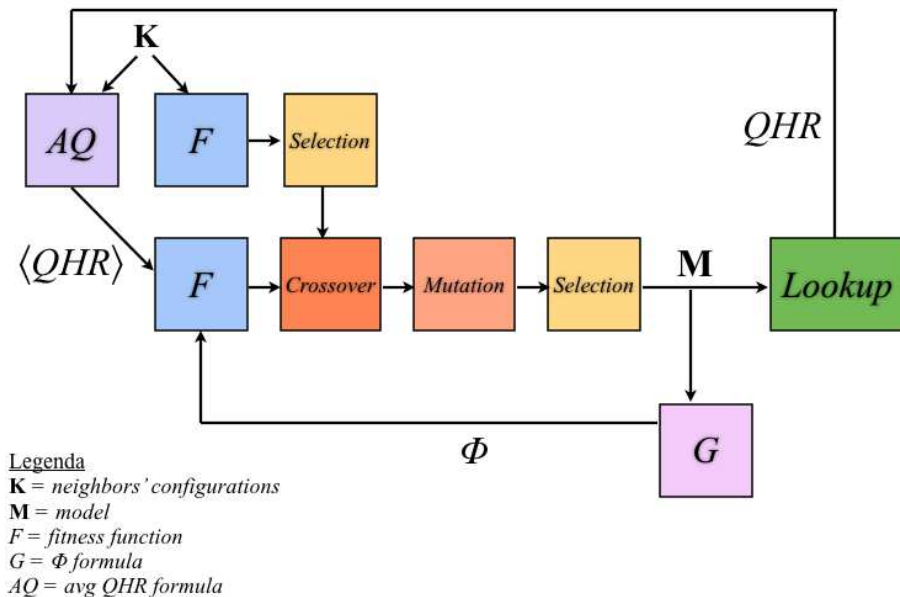


Figure 2: Functional architecture of the peer.

the neighbors.

Algorithm 2 may appear too complicated, for the relatively simple model that is used. Alternatively, each peer may test all the possible configurations on its own, and use the one having best fitness. However, in this way, the time required before a group of linked peers reached the optimal configuration for the local environment would probably be longer. Another possible strategy could be to compare the local model with those of the neighbors, and select the best one, without using crossover and mutation. However, this could lead to non-optimal configurations of the whole network, as the considered problem domain may have a complex fitness landscape, depending on the specific characteristics of the network itself.

5 Simulations

To evaluate the performance of the proposed ultra-large-scale system, we used a general-purpose discrete event simulation environment, called DEUS, based on Java and XML, released as open source under the GPL license [33]. Such a tool has been used instead of classical network simulators (*e.g.*, ns-2

Algorithm 2 Adaptation

```
1: let  $g = 0$ 
2: while not converged do
3:   evaluate the fitness of own model
4:    $g = g + 1$ 
5:   select neighbor with best fitting model
6:   perform cross-over with best neighbor to generate offspring  $\mathcal{O}_g = \{\mathbf{O}_{g1}, \mathbf{O}_{g2}\}$ 
7:   mutate offspring in  $\mathcal{O}_g$  with probability  $1 - \langle QHR \rangle$ 
8:   select the new generation  $\mathcal{M}_g$  from the previous generation  $\mathcal{M}_{g-1}$  and the offspring  $\mathcal{O}_g$ 
9: end while
```

or Opnet), since it is optimized to analyze P2P networks at a higher level. In particular, with DEUS it is possible to simulate highly dynamic overlays (*i.e.* application level) networks, with several hundred thousands nodes, on a single machine — without the need to simulate also lower network layers (whose effect can be taken into account, in any case, when defining the virtual time scheduling of message propagation events). With respect to PeerSim, a highly reliable simulation tool specifically designed for simulating peer-to-peer networks [34], the approach of DEUS is much simpler, in general: the user just need to extend three classes to define his/her own events, nodes and time-regulating processes. Everything else is managed by the simulation engine.

Each simulated peer is characterized by three kinds of consumable resources: CPU, RAM, and disk space. Their values are randomly generated (with uniform distribution) as multiple of, respectively, 512 MHz, 256 MB, and 10 GB. The maximum amount of resources per peer is 2 GHz, 1 GB for the RAM, and 100 GB for the disk space.

We assumed $M_i \in [1..6]$ ($n = 6$), and we set

- $f_k = M_0/6$
- $T_{max} = M_1$
- $D_{max} = 2M_2$

to have reasonable values. Regarding f_k , that choice is mandatory because it must be in $[0, 1]$.

The phenotype Φ is obtained by means of (6), with $\phi_0 = 100$, $\phi_1 = 10$, and $\phi_2 = 5$. With these weight values, f_k has more importance than T_{max}

and D_{max} in the computation of the fitness value. The average query hit ratio $\langle QHR \rangle$ is given by (7). To avoid biasing, the initial QHR value for every peer is 0.5.

We compared the effects of the fitness functions F_2 and F_4 (defined in section 4), that are substantially different because the second one is characterized by a threshold under which $\langle QHR \rangle$ is considered to be bad, while the first one has no explicit constraints.

All the experiments were carried out with a simulated P2P network of $N = 10000$ nodes, with a topology constructed without preferential attachment, starting from N_0 completely connected nodes, and each other peer being attached to $m \in [1, N_0]$ existing peers, with even probability. All connections are bidirectional, *i.e.* if node n_a has node n_b in its peerview, then n_b has n_a in its peerview. The resulting degree distribution is exponential:

$$P(k) = (1 - e^{-\frac{1}{m}})e^{(1-\frac{k}{m})} \quad \forall k \geq m$$

with expected value

$$E(k) = \sum_{k=m}^{\infty} kP(k) = \frac{e^{(1-\frac{1}{m})}}{1 - e^{-\frac{1}{m}}}$$

In these experiments, we used the typical values $m = 3$ and $N_0 = 5$ [35]. After the initial topology has been constructed, network churn is simulated. Node departures and joins are modeled by means of two Poisson processes with the same rate $\lambda_1 = 0.14 \text{ s}^{-1}$, for which the average network size remains $N = 10000$.

We considered two scenarios: *static load* and *changing load*. In the former, we simulated 150 minutes of the life of a network of peers, with resource queries occurring continuously and independently of one another — according to a Poisson process with parameter $\lambda_2 = 0.028 \text{ s}^{-1}$, *i.e.* 36 queries every second, each one associated to a randomly chosen node. Each query is a request for a randomly generated amount of resources (no more than 2 GHz of CPU, 1 GB of RAM, and 100 GB of disk space, respectively). Once a resource has been found, it is consumed for a random time interval (according to an exponential distribution with mean value 280 s — for which the system’s utilization would be 1, if a provider was found for every request).

In the second scenario (changing load), we still simulated 150 minutes of the life of a network of peers, but we considered a load on system changing

over time. In the first 50 minutes, almost all resource queries ask for 2 GHz, 1 GB of RAM, and 100 GB of disk space (like in previous experiments). In the following 100 minutes the load is reduced, with almost all resource queries asking for 256 MHz, 128 MB of RAM, and 1 GB of disk space.

Every node performs adaptation every T_a seconds, for both fixed and noisy networks. All the following results refer to experiments with $T_a = 7$ seconds. Fig. 3 illustrates how the settling time t_s is affected by the adaptation period, for the static load scenario. Here, the settling time is defined as the time required for the response curve to reach and stay within a range of 5% percentage of the final value. We observe that F_4 is always better than F_2 , for any value of T_a . Moreover, it is evident that $T_a = 7$ is a good choice for F_4 , since lower values would not be very beneficial for the settling time, while higher values would increase it too much. The exchange of control messages between each node and its neighbors, to support the adaptation process, produces negligible bandwidth consumption, since only the models \mathbf{M} are exchanged (and each node has few neighbors). As already stated before, the adaptation process at the level of each node has a limited computational overhead. However, T_a could be considered as part of the phenotype, and mapped into the model \mathbf{M} , in order to be dynamically updated depending on the evaluated performance of the peer. This approach will be evaluated in a future work.

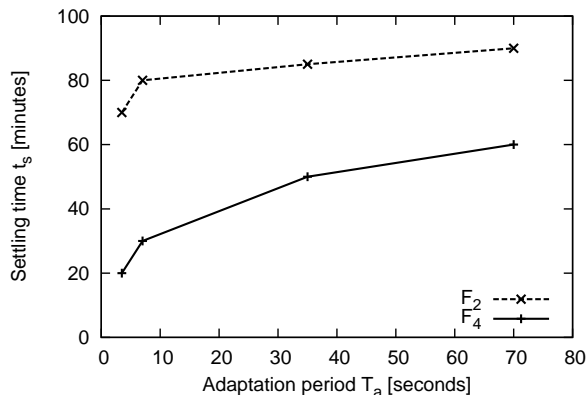


Figure 3: Settling time t_s versus adaptation period T_a in the "static load" scenario, comparing fitness functions F_2 and F_4 .

For each scenario and fitness function (F_2 and F_4), we executed 25 sim-

ulations, each one with a different seed for the random number generator. Reported values in the graphs are the averaged values of such simulations. In each simulation run, the global QHR value is obtained by averaging on all the nodes of the network. The standard deviation also refers to such averaging, which is performed during the simulation, at regular intervals. The same approach has been applied for measuring also the global values of $M_i \forall i \in [0, 2]$, E , S , C and H .

Figures 4 and 5 illustrate the average evolution of \mathbf{M} and QHR over time, for each considered fitness function, in the static load scenario.

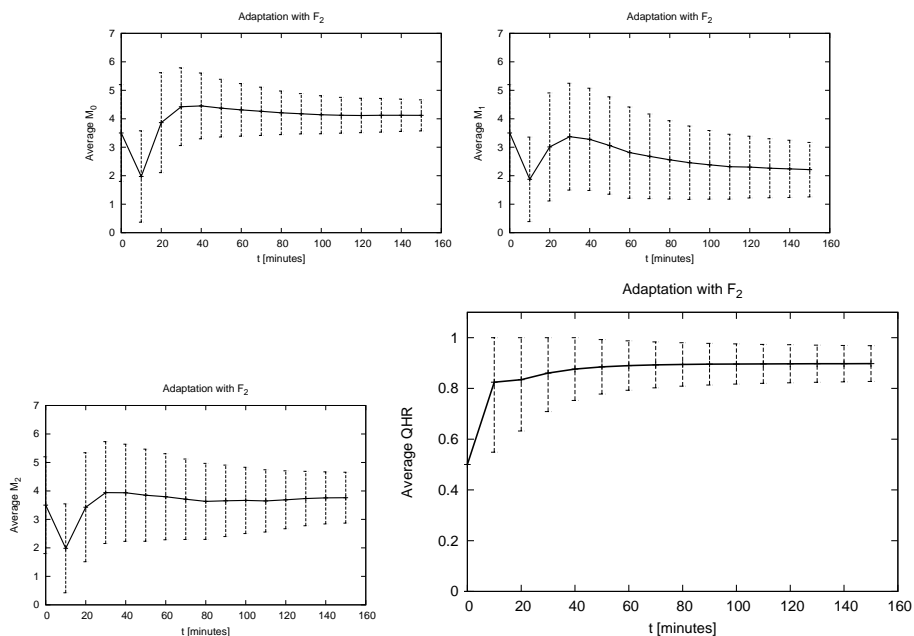


Figure 4: Average M_0 , M_1 , M_2 and QHR over time, for fitness function F_2 . The load on the system is static.

For the average global QHR , we have computed the 95% confidence interval and performed the Wilcoxon rank-sum test. In details, we have considered the two sets of 25 samples each, representing the global QHR at time $t = 150$ minutes, when fitness functions F_2 and F_4 are used. Table 1 shows that, for the scenario with static load, with F_2 , the values of the global QHR fall in the interval $I_{95} = [0.8548; 0.9406]$; with F_4 , they fall in $I_{95} = [0.8898; 0.9115]$. In the same scenario, the Wilcoxon rank-sum test says that the distribution of the global QHR , when F_2 is used, has the same expected mean value than

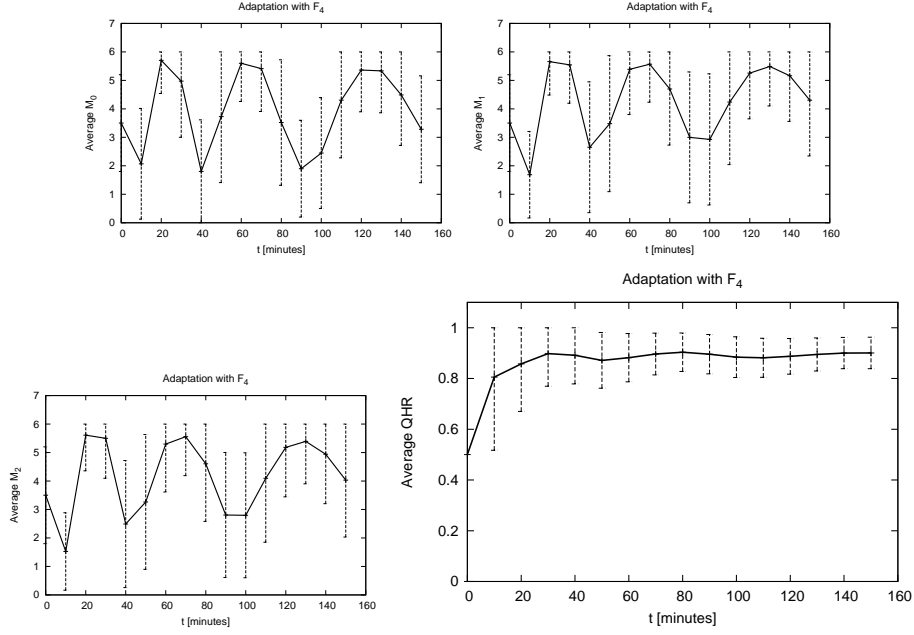


Figure 5: Average M_0 , M_1 , M_2 and QHR over time, for fitness function F_4 . The load on the system is static.

the one we obtain when F_4 is used. The p-value is $0.272 > 0.05$, which means that the null hypothesis

H_0 : the median value of the distribution of the outputs from F_2 equals the median value of the distribution of the outputs from F_4

is confirmed. The second row of the table shows the analysis of the standard deviation of the global QHR , which is higher with F_2 than with F_4 .

Statistical analysis							
Variable	μ_{F_2}	σ_{F_2}	μ_{F_4}	σ_{F_4}	$I95_{F_2}$	$I95_{F_4}$	p-value ($F_2 = F_4$)
avg global QHR	0.8977	0.0207	0.9	0.0052	[0.8548; 0.9406]	[0.8898; 0.9115]	0.272
std dev global QHR	0.0705	0.0087	0.0621	0.0033	[0.0523; 0.0886]	[0.0551; 0.0691]	$5 \cdot 10^{-4}$

Table 1: Adaptation with static load (25 samples $\forall F_i$)

The same characterization, for the scenario with changing load, is reported by Fig.6 and Fig.7.

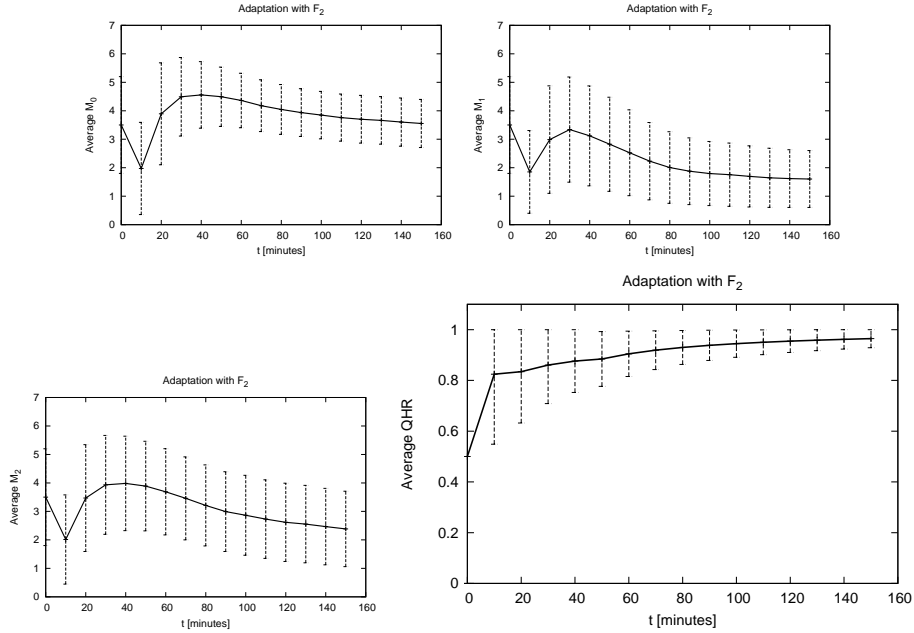


Figure 6: Average M_0 , M_1 , M_2 and QHR over time, for fitness function F_2 . The load on the system changes at minute 50.

Table 2 shows that in this scenario (dynamic load), the global QHR has higher mean value and lower standard deviation (computed over the 25 runs) if F_2 is used. The fact that F_2 leads to better results than F_4 , over multiple simulation runs, is confirmed by the $I95$ and rank-sum analyses. Once more, we recall that this particular observation refers only to the "stable value" of the global QHR , and the performance analysis must be completed by observing the transient phases. It is evident, from figures 6 and 7, that F_4 leads to a more responsive system, with respect to F_2 . This is further discussed below.

In general, when QHR decreases for most peers, the system reacts in a way that chromosomes with higher gene values survive and proliferate. Both the considered fitness functions make the genes M_i change over time (with

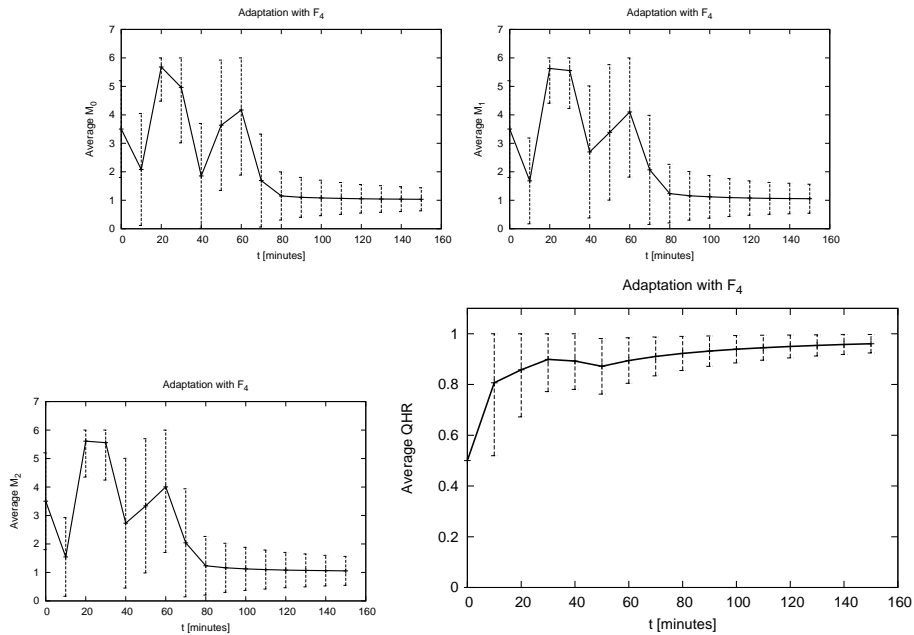


Figure 7: Average M_0 , M_1 , M_2 and QHR over time, for fitness function F_4 . The load on the system changes at minute 50.

Statistical analysis							
Variable	μ_{F_2}	σ_{F_2}	μ_{F_4}	σ_{F_4}	$I95_{F_2}$	$I95_{F_4}$	p -value ($F_2 > F_4$)
avg global QHR	0.9646	0.0019	0.9606	$8 \cdot 10^{-4}$	[0.9606; 0.9687]	[0.9589; 0.9623]	$1 \cdot 10^{-8}$
std dev global QHR	0.036	0.0013	0.0364	$5 \cdot 10^{-4}$	[0.0332; 0.0387]	[0.0352; 0.0376]	0.8

Table 2: Adaptation with changing load (25 samples $\forall F_i$)

an initial transient phase), to maximize the QHR . Because of node departures and arrivals, the genes are characterized by high standard deviation. The reason is that joining and leaving nodes introduce random chromosomes that produce the same effect as mutation. With F_4 the standard deviation of the genes is particularly high, because of the firm threshold β which characterizes F_4 : if $\langle QHR \rangle$ oscillates around β , the genes do not reach a stable configuration. However, this produces a positive effect on the global QHR .

In the second scenario, with changing load, both the considered fitness functions make the genes M_i increase in the first period (high load), and decrease in the second period (reduced load). We notice that F_4 leads to a

more prompt reaction, *i.e.* gene values decrease almost immediately when the environmental conditions change. Such a reactive behavior is highly appreciated, considering the large size of the system.

We measured also the evolution over time of the information I associated to the current genotype \mathbf{M} , according to the procedure illustrated in section 3. Figures 8 to 11 are related to the case of $W = 1$.

For the static load scenario, F_2 produces balanced change in time, reflected in medium E and S and a high C . F_4 offers less change on average, as seen by a higher S and H , lower E , and medium C . Still, the rate of information change changes considerably in time, leading to a variance in the measures, especially high for C .

For the changing load scenario, F_2 performs in a similar fashion: it is not able to adapt to the reduction of the demand. Conversely, F_4 does adapt at the demand change at minute 50, stabilizing at minute 80. This is seen in maximal S and H and minimal E and C , indicating that there is no change in the nodes. This is because of the threshold used in F_4 .

Higher S and H imply static behavior, which might be desired after the load change, in the second scenario. High E implies change, while a high C implies a balance between S and E , *i.e.* adaptivity. A high C is desirable when changes are being made to the load, not when there are no changes.

6 Conclusion

We proposed the use of measures based on information theory to study the performance of ULS systems. These measures are general enough to be used with any proposed ULS, enabling comparison between different approaches.

We presented simulation results of an ULS computing system with two different types of genetic adaptation while measuring their complexity, emergence, self-organization and homeostasis. The main result is that less "aggressive" adaptive plans lead to a more stable system, but the optimal performance may not be achieved.

Future work will follow two main directions. Firstly, with respect to the use case proposed in this paper, we will study the impact of parameter variations and we will consider also other workload profiles. Then, we will generalize the analysis to the case of systems with components that dynamically change their structure, by removing or adding components.

References

- [1] L. Northrop, P. Feiler, R. P. Gabriel, J. Goodenough, R. Linger, T. Longstaff, R. Kazman, M. Klein, L. Northrop, D. Schmidt, K. Sullivan, K. Wallnau, Ultra-Large-Scale Systems: The Software Challenge of the Future, Carnegie Mellon Software Engineering Institute, Ultra-Large-Scale Systems Study Report, 2006.
- [2] C. Gershenson, F. Heylighen, How Can We Think the Complex?, in: K. Richardson (Ed.), *Managing Organizational Complexity: Philosophy, Theory and Application*, Information Age Publishing, Charlotte, 2005, pp. 47–61. <http://arxiv.org/abs/nlin.AO/0402023>
- [3] C. Gershenson, The Implications of Interactions for Science and Philosophy, *Foundations of Science*, in press. <http://arxiv.org/abs/1105.2827>
- [4] C. Gershenson, *Design and Control of Self-organizing Systems*, CopIt Arxiv, Mexico, 2007.
- [5] H. Psai, S. Dustdar, A survey on self-healing systems: approaches and systems, *Computing*, 91 (1) (2011) 43–73.
- [6] S. Dobson, R. Sterritt, P. Nixon, M. Hinchey, Fulfilling the Vision of Autonomic Computing, *IEEE Computer Magazine* 43 (1) (2010) 35–41.
- [7] C. Gershenson and N. Fernandez, Complexity and Information: Measuring Emergence, Self-organization, and Homeostasis at Multiple Scales, *Complexity* 18 (2) (2012) 29–44.
- [8] M. Amoretti, Introducing Artificial Evolution into Peer-to-Peer Networks with the Distributed Remodeling Framework, *Genetic Programming and Evolvable Machines*, in press, doi:10.1007/s10710-013-9182-0.
- [9] K. C. Foo, Z. M. Jiang, A. E. Hassan, Y. Zou, K. Martin, P. Flora, Modeling the performance of Ultra-Large-Scale systems using layered simulations, *IEEE Int. Workshop on the Maintenance and Evolution of Service-Oriented and Cloud-Based Systems (MESOCA 2011)*, Williamsburg, VA, USA, September 2011.
- [10] IBM, An architectural blueprint for autonomic computing. Tech. rep. (2003).

- [11] M. C. Huebscher, J. A. McCann, A survey of autonomic computing — degrees, models, and applications, *ACM Computing Surveys* 40 (3) (2008).
- [12] C. Müller-Schloer, H. Schmeck, Organic Computing - Quo Vadis?, in: C. Müller-Schloer, H. Schmeck, T. Ungerer (Eds.), *Organic Computing — A Paradigm Shift for Complex Systems*, Birkhäuser Verlag, 2011, pp. 615–627.
- [13] R. Bruni, A. Corradini, F. Gadducci, A. Lluch Lafuente, A. Vandin, A Conceptual Framework for Adaptation, *Proc. of the 15th Int.'l Conf. on the Fundamentals of Software Engineering (FASE'12)*, LNCS 7212, Springer, 2012, pp. 240–254.
- [14] T. Nakano, T. Suda, Self-Organizing Network Services With Evolutionary Adaptation, *IEEE Trans. on Neural Networks* 16 (5) (2005) 1269–1278.
- [15] D. Hales, From Selfish Nodes to Cooperative networks — Emergent Link-based incentives in Peer-to-Peer Networks, *Proc. 4th IEEE Intl Conf. on Peer-to-Peer Computing*, Zurich, Switzerland, 2004.
- [16] G. Tyson, P. Grace, A. Mauthe, S. Kaune, The Survival of the Fittest: An Evolutionary Approach to Deploying Adaptive Functionality in Peer-to-Peer Systems, *Proc. of the 7th Workshop on Reflective and Adaptive Middleware*, Leuven, Belgium, 2008.
- [17] M. Amoretti, A Survey of Peer-to-Peer Overlay Schemes: Effectiveness, Efficiency and Security, *Recent Patents on Computer Science* 2 (3) (2009) 195–213.
- [18] B. F. Cooper, H. Garcia-Molina, SIL: A model for analyzing scalable peer-to-peer search networks, *Computer Networks* 50 (13) (2006) 2380–2400.
- [19] M. Karakaya, I. Korpeoglu, O. Ulusoy, Counteracting free riding in Peer-to-Peer networks, *Computer Networks* 52 (3) 22 (2008) 675–694.
- [20] F. Esposito, I. Matta, D. Bera, P. Michiardi, On the impact of seed scheduling in peer-to-peer networks, *Computer Networks* 55 (15) (2011) 3303–3317.

- [21] Y. Chen, E. Le Merrer, Z. Li, Y. Liu, G. Simon, OAZE: A network-friendly distributed zapping system for peer-to-peer IPTV, *Computer Networks* 56 (1) (2012) 365–377.
- [22] L. Onana Alima, S. El-Ansary S, P. Brand, S. Haridi, DKS(N,k,f): A family of low communication, scalable and fault-tolerant infrastructures for p2p communications, *Proc. of the 3rd IEEE/ACM Inter Symposium on Cluster Computing and the Grid (CCGRID '03)*, Tokyo, Japan, 2003.
- [23] B. Paechter, T. Back, M. Schoenauer, M. Sebag, A. E. Eiben, J. J. Merelo, T. C. Fogarty, A distributed resource evolutionary algorithm machine (DREAM), *Proc. IEEE Congress on Evolutionary Computation (CEC 2000)*, IEEE, 2000, pp.951–958.
- [24] M. Prokopenko, F. Boschetti and A. J. Ryan An Information-Theoretic Primer On Complexity, Self-Organisation And Emergence, *Complexity*, 15 (1) 11–28.
- [25] C. Langton, Computation at the edge of chaos: Phase transitions and emergent computation, *Physica D* 42 (1990) 12–37.
- [26] S. A. Kauffman, *The Origins of Order*, Oxford University Press, 1993.
- [27] C. Gershenson, The World as Evolving Information, *International Conference on Complex Systems (ICCS 2007)*, <http://arxiv.org/abs/0704.0304>.
- [28] C. Gershenson and F. Heylighen, When can we call a system self-organizing?, In W. Banzhaf, T. Christaller, P. Dittrich, J. T. Kim, J. Ziegler (Eds.), *Advances in Artificial Life, 7th European Conference (ECAL 2003)*, LNAI 2801, Springer, 2003, pp. 606–614.
- [29] P.T. Eugster, R. Guerraoui, A.-M. Kermarrec, L. Massoulié, *From Epidemics to Distributed Computing*, *IEEE Computer*, Vol. 37, No. 5, May 2004.
- [30] E. Ahi, M. Caglar, O. Ozkasap, Stepwise Fair-Share Buffering underneath Bio-inspired P2P Data Dissemination, *Proc. 6th International Symposium on Parallel and Distributed Computing (ISPDC'07)*, IEEE, Hagenberg, 2007, p. 177–184.

- [31] The Gnutella Developer Forum (GDF), The Annotated Gnutella Protocol Specification v0.4, <http://rfc-gnutella.sourceforge.net/developer/stable/index.html>
- [32] J. L. Laredo, A. E. Eiben, M. Steen, J. J. Merelo, EvAg: a scalable peer-to-peer evolutionary algorithm, *Genetic Programming and Evolvable Machines* 11(2) (2010) pp. 227–246.
- [33] M. Amoretti, M. Agosti, F. Zanichelli, DEUS: a Discrete Event Universal Simulator, *Proc. of the 2nd International Conference on Simulation Tools and Techniques (SIMUTools 2009), ICST/ACM, 2009.*
- [34] A. Montresor, M. Jelasity, PeerSim: A scalable P2P simulator, *Proc. of the 9th Int. Conference on Peer-to-Peer (P2P'09), IEEE, pp. 99–100.*
- [35] A.-L. Barabasi, R. Albert, Emergence of Scaling in Random Networks, *Science* 286 (1999).

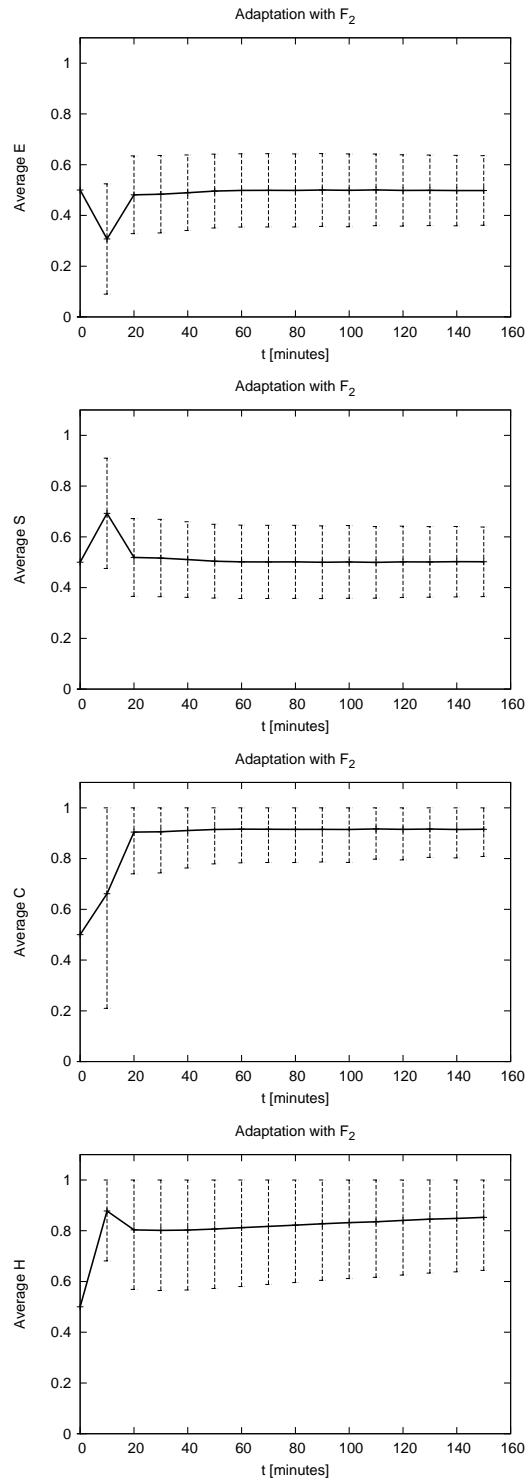


Figure 8: Average E , S , C and H ²⁵ over time, for fitness function F_2 . The load on the system is static.

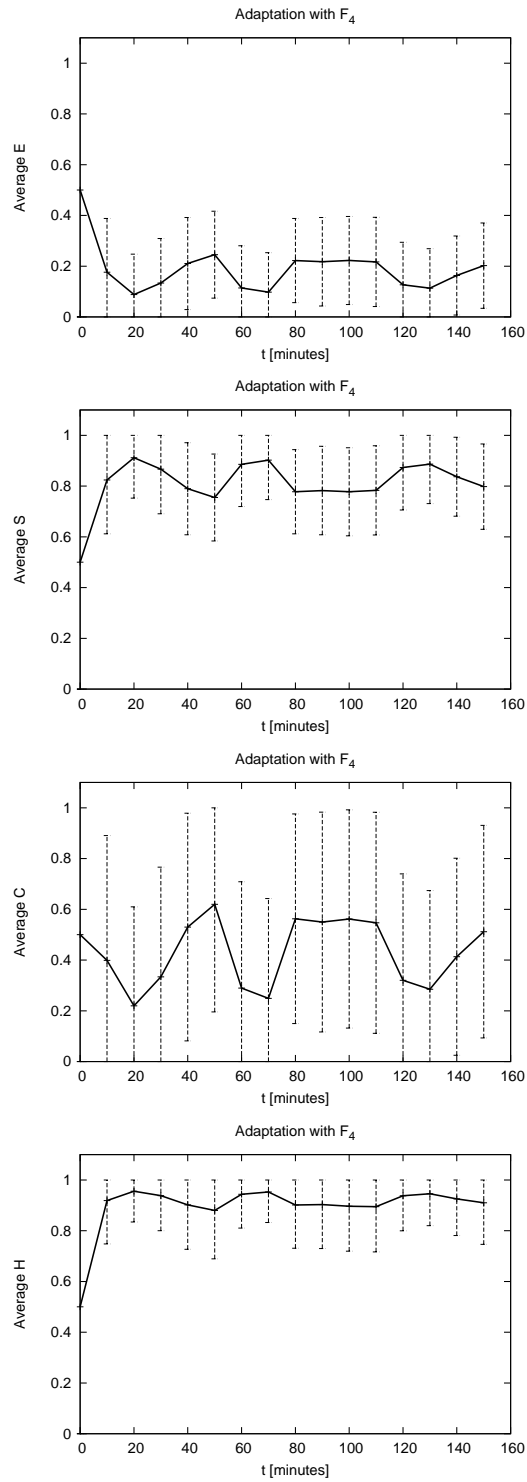


Figure 9: Average E , S , C and H ²⁶ over time, for fitness function F_4 . The load on the system is static.

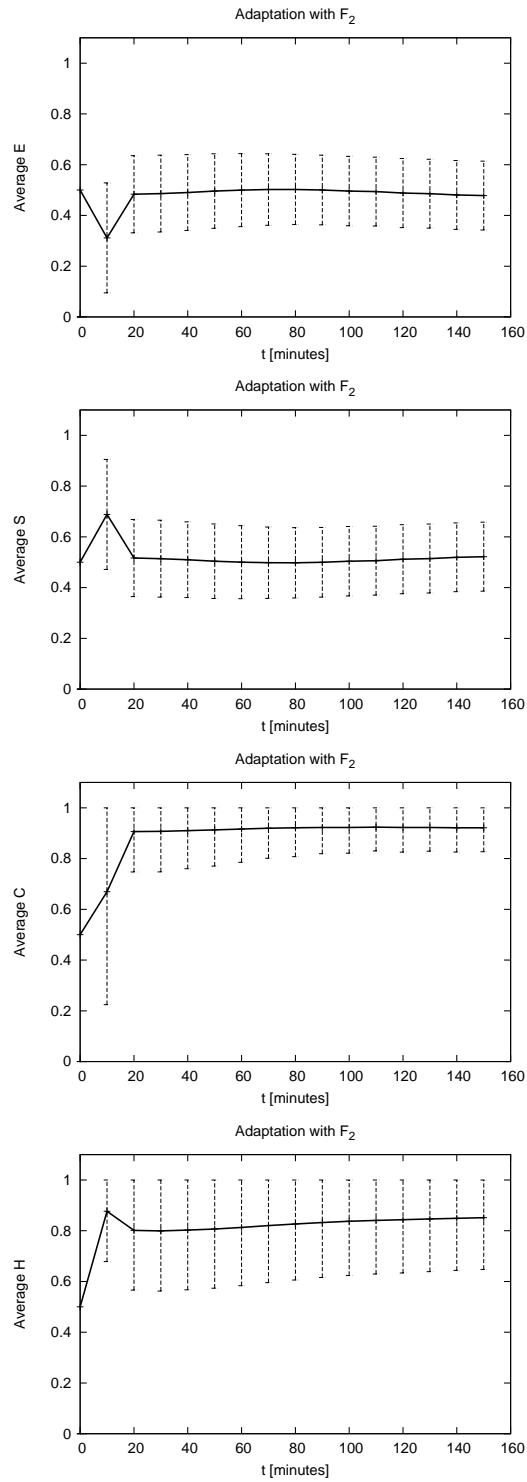


Figure 10: Average E , S , C and H ²⁷ over time, for fitness function F_2 . The load on the system changes at minute 50.

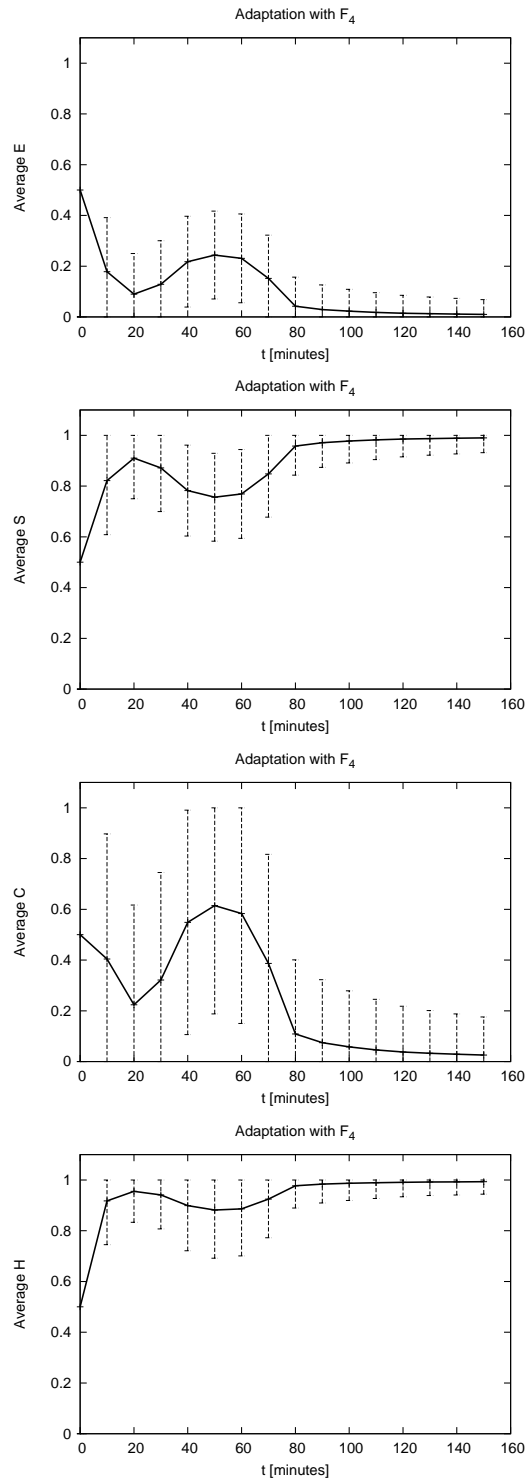


Figure 11: Average E , S , C and H ²⁸ over time, for fitness function F_4 . The load on the system changes at minute 50.

This figure "overlayLM.jpg" is available in "jpg" format from:

<http://arxiv.org/ps/1207.6656v2>